# New Diphenylacetylenes as Probes for Positron Emission Tomographic Imaging of Amyloid Plaques

Rajesh Chandra,[†] Shunichi Oya,[†] Mei-Ping Kung,[†] Catherine Hou,[†] Lee-Way Jin,[‡] and Hank F. Kung*[,†,§]

*Departments of Radiology and Pharmacology, University of Pennsylvania, Philadelphia, Pennsylvania 19104, and Department of Pathology, University of California Health System, Sacramento, California 95817*

*Received January 23, 2007*

A series of $^{18}$F fluoropegylated diphenylacetylenes as probes for binding to A$\beta$ plaques were successfully prepared. These relatively rigid acetylenes, **12a**, **12b**, **14a**, and **14b**, displayed high binding affinities in postmortem AD brain homogenates ($K_i$ ranging from 1.2 to 2.9 nM). In vivo biodistribution in normal mice exhibited excellent initial brain penetrations (4.42, 4.55, 5.41, and 6.78% dose/g at 2 min for [$^{18}$F]**12a**, **12b**, **14a**, and **14b**, respectively). [$^{18}$F]**12b** and [$^{18}$F]**14b**, with a longer fluoropegylated unit, that is, $n = 3$, showed faster brain washout at 30 min postinjection (0.42 and 1.57% dose/g) as compared to the shorter fluoropegylated chain ligands, that is, [$^{18}$F]**12a** and [$^{18}$F]**14a** (1.03 and 3.69% dose/g). Autoradiography and homogenate binding confirmed the high binding signal due to A$\beta$ plaques. These preliminary results suggest that the novel diphenylacetylenes may be potentially useful for imaging of A$\beta$ plaques in the brain of patients with Alzheimer's disease.

## Introduction

Alzheimer's disease (AD[a]) is a neurodegenerative disease affecting millions of elder people. Major neuropathology observations of postmortem AD brains depict the presence of senile plaques (containing $\beta$-amyloid (A$\beta$) aggregates) and neurofibrillary tangles (highly phosphorylated tau proteins). The exact mechanisms leading to the development of AD are not fully understood, however, the formation of A$\beta$ plaques, consisting of $\beta$-sheets of A$\beta$ protein aggregates, in the brain is a pivotal event in the pathology of Alzheimer's disease.[1−7] Developing specific probes for in vivo imaging studies of A$\beta$ plaques may be important for the diagnosis and monitoring of AD patients.[1,8−11] The imaging technique could improve diagnosis by identifying potential patients with A$\beta$ plaques in the brain that are likely to develop AD. When antiplaque drug treatments become available, the imaging of A$\beta$ plaques in the brain may serve as an essential tool for monitoring the progression and the treatment of the disease.

Development of A$\beta$ plaque-specific imaging agents has been reported previously (for review see refs 10−14). Different PET (positron emission tomography) and SPECT (single photon emission tomography) tracers, such as [$^{11}$C]PIB, **1**,[15] [$^{11}$C]SB-13, **2**,[16] [$^{18}$F]FDDNP, **3**,[17,18] and [$^{123}$I]IMPY, **4**,[19] have been tested clinically and demonstrated the potential utility of in vivo imaging of A$\beta$ plaque deposition in the brain. Using PIB/PET to study the relationship between A$\beta$ plaque burden and AD neurological measurements, the results seem to suggest that there are some mild cognitive impairment cases that convert to AD, while those with lower PIB uptake in the cortex appear to have less propensity to convert to AD.[20−22] Additional tracers labeled with $^{18}$F ($T_{1/2} = 110$ min, $\beta^+$, commonly produced by a cyclotron) may be even more useful as PET imaging agents for detection and quantification of A$\beta$ aggregates since the half-life of $^{18}$F (110 min) is 5.5 times longer than $^{11}$C ($T_{1/2} = 20$ min, $\beta^+$). Using $^{18}$F tracers, the manufacturing and distribution can be centralized, which will significantly simplify the clinical application.

A highly lipophilic tracer, [$^{18}$F]FDDNP, **3** (Figure 1), for binding to both tangles and plaques has been reported.[23] Preliminary studies in humans suggested that [$^{18}$F]FDDNP showed a higher retention in regions of the brain suspected of having tangles and plaques,[17,24−26] therefore, it is not selective for measuring A$\beta$ burden in the AD brain. Fluorinated PIB and related neutral thioflavin derivatives, such as BTA-1, have also been reported.[11,27] However, clinical studies of the $^{18}$F-labeled PIB have not yet been published in a full paper.

We have recently prepared potential PET imaging probes based on stilbene, **5**, and styrylpyridines,[28−30] **6**, (see Figure 1). The fluoropegylated group or simply an ethylene glycol group was retained to reduce the lipophilicity and maintain neutrality. As part of the continuing effort in developing probes for imaging A$\beta$ plaques in the brain, we have prepared a series of fluoropegylated diphenylacetylenes, which mimic the structure of fluoropegylated stilbenes. The diphenylacetylene derivatives employed in the present study are a simplified version of SB-13, **2**; the double bond in the SB-13, **2**, is replaced by a triple bond. Two reasons prompted us to investigate this class of compounds. They can be synthesized by Sonogashira reaction, which is tolerant to a wide variety of functional groups. The second and more important reason is the nonexistence of geometrical isomers, which is an often-encountered problem with their double-bonded counterparts.[31] The diphenylacetylenes are relatively rigid; therefore, the degree of freedom around the triple bond is limited, leading to a tight fit to the binding pocket at the $\beta$-sheets. An additional impetus came from the fact that none of the A$\beta$ plaque imaging agents so far reported have been based on a triple-bonded (diphenylacetylene) structure.

* To whom correspondence should be addressed. Hank F. Kung, Ph.D., Department of Radiology, University of Pennsylvania, 3700 Market Street, Room 305, Philadelphia, PA 19104. Tel.: (215) 662-3096. Fax: (215) 349-5035. E-mail: kunghf@sunmac.spect.upenn.edu.

[†] Department of Radiology, University of Pennsylvania.

[‡] Department of Pathology, University of California Health System.

[§] Department of Pharmacology, University of Pennsylvania.

[a] Abbreviations: SPECT, single photon emission computed tomography; PET, positron emission tomography; AD, Alzheimer's disease; MCI, mild cognitive impairment; A$\beta$, $\beta$-amyloid; PIB, 2-(4′-(methylaminophenyl)-6-hydroxybenzothiazole; SB-13, 4-*N*-methylamino-4′-hydroxystilbene; FDDNP, 2-(1-{6-[(2-fluoroethyl)methyl-amino]-2-naphthyl}ethylidend)-malononitrile; IMPY, 6-iodo-2-(4′-dimethylamino-)phenyl-imidazo[1,2-*a*]pyridine.

10.1021/jm070090j CCC: $37.00 
Published on Web 04/21/2007

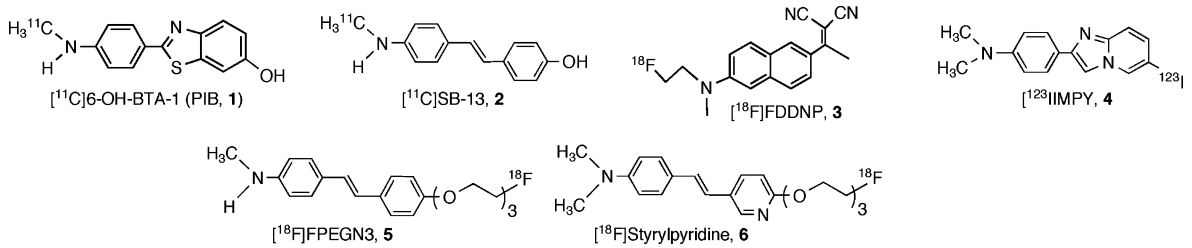


**Figure 1.** Chemical structures of various probes previously reported for imaging A$\beta$ aggregates.

The desired diagnostic imaging agents of AD based on A$\beta$ plaque-specific binding can be defined as ligands with the following properties: (a) high binding affinity to A$\beta$ aggregates; $K_i$ < 10 nM; (b) high binding selectivity; $K_i$ for other sites > 100-fold; (c) readily labeled with nuclide for imaging; (d) small (mol wt < 600), lipophilic (P.C. = 100−1000) and neutral molecules; (e) desirable pharmacokinetics; good initial brain uptake (>4% dose/g at 2 min post iv injection in normal mice) and fast washout (less than 30% of initial uptake remaining at 30 min in the brain of normal mice); (f) in vivo stability as evaluated by in vitro metabolism studies (metabolite in the brain is less than 5% of parent ligand).

Initially, we have prepared limited *p*-*N*,*N*-dimethylamino-diphenylacetylene derivatives, which have not been reported previously, to see if they showed reasonably good binding affinities toward A$\beta$ plaques. Once it became apparent that suitably substituted diphenylacetylene structures indeed showed excellent binding to A$\beta$ plaques in vitro, we proceeded to synthesize fluorine-containing derivatives. These molecules have two distinct parts, planar or easily planarized diphenylacetylene, bearing a nucleophilic group ($NH_2$, NHMe, $NMe_2$, OH, or OMe) for binding and the second part containing a fluoropolyethyleneglycol (FPEG) for carrying the radio tracer, [$^{18}$F]fluorine, in the present study. It is also worth mentioning that the lipophilicity of these molecules could be fine-tuned by varying the length of the PEG chain until a molecular weight ceiling of 600 Da is reached. We herein report a series of $^{18}$F-labeled diphenylacetylenes as PET imaging probes for detecting A$\beta$ plaques in the brain.

## Experimental Section

**General Methods.** $^1$H NMR spectra were recorded on Bruker DPX 200 MHz spectrometer in $CDCl_3$ or $CD_3OD$, chemical shifts were reported as $\delta$ values with respect to residual solvent protons unless otherwise mentioned. The coupling constants (*J*) were reported in Hz. The multiplicity is defined by s (singlet), d (doublet), t (triplet), br (broad), and m (multiplet). High-resolution mass spectrometry (HRMS) was performed at the McMaster Regional Centre for Mass Spectrometry, McMaster University, using a micromass/Waters GCT instrument (GC-EI/CI time-of-flight mass spectrometer). The microwave reactions were carried out in biotage initiator microwave synthesis system. Commercially available reagents were used as received without further purification. Crude products were purified by either flash chromatography using 230−400 mesh silica gel (Aldrich grade 9385, 60 Å) or preparative TLC (Analtech, 20 × 20 cm, 2000 microns). The reported chemical yields were not optimized. The purities of compounds **9**(**a**,**b**), **11**(**a**,**b**), **12**(**a**,**b**), **14**(**a**,**b**), **17**, **19b**, **20**(**a**,**b**), and **23**(**a**,**b**), which were used for biological evaluations, were determined using both reverse phase and normal phase HPLC (Agilent 1100 series LC), and all of them were determined to be >95% pure. Analytical HPLC was performed using a Hamilton PRP-1 reverse phase column (4.1 × 250 mm, 10 $\mu$m) eluted with an acetonitrile/aq buffer (1 mM ammoniumformate, pH 7) mobile phase mixture or a Phenomenex Silica normal phase column (4.6 × 250 mm, 5 $\mu$m) eluted with an ethylacetate/hexane mobile phase mixture. Both columns were eluted at flow rates of 1.0 mL/min. The chromatographic systems were fitted with UV detectors set at 280 nm.

**General Procedure for Sonogashira Reaction: Method A:** This procedure is followed when the acetylene used in the reaction is 4-ethynylaniline (**7a**). To a mixture of $PdCl_2(PPh_3)_2$ (1 mol % with respect to iodoarene), CuI (2 mol % wrt iodoarene), and iodoarene (0.5 mmol) in 3 mL of anhyd THF (degassed with argon) was added, at room temperature under argon, 4-ethynylaniline **7a** (0.6 mmol). Ammonia solution (0.5 M aq; 2 mL, 1 mmol) was then added dropwise, and the mixture was stirred at room temperature for 4 h. Diethyl ether (20 mL) and water (20 mL) were then added to the reaction. The organic layer was separated and the aqueous layer was further extracted with ether (3 × 10 mL). The combined organic layer was dried ($MgSO_4$) and concentrated, and the residue was purified by silica gel column chromatography (appropriate mixture of hexane−ethyl acetate).

**Method B:** This procedure is followed when the acetylene used in the reaction is 4-ethynyl-*N*,*N*-dimethylaniline (**13**). A mixture of $PdCl_2(PPh_3)_2$ (2 mol % with respect to iodoarene), CuI (2 mol % wrt iodoarene), and iodoarene (0.5 mmol) were taken in a round-bottomed flask equipped with a reflux condenser, and the whole set up was degassed and back-filled with a gaseous mixture of approximate 1:1 $H_2$ and Ar. THF followed by TEA were then syringed in and the mixture was heated to 60 °C. A solution of 4-ethynyl-*N*,*N*-dimethylaniline (0.5 mmol) in 2.5 mL of THF was then added under the reducing atmosphere of 1:1 $H_2$ and Ar. After refluxing the mixture for 16 h, the solvents were evaporated and the residue was purified by silica gel column chromatography (appropriate mixture of hexane−ethyl acetate).

**4-(4-Amino-phenylethynyl)-phenol (9a).** Compound **9a** was prepared according to method A: yield 54%. $^1$H NMR (200 MHz, $CD_3OD$, $\delta$ ppm): 6.64 (d, *J* = 8.7 Hz, 2H), 6.74 (d, *J* = 8.8 Hz, 2H), 7.18 (d, *J* = 8.7 Hz, 2H), 7.27 (d, *J* = 8.8 Hz, 2H). HRMS calcd for $C_{14}H_{11}NO$ ($M^+$), 209.0841; found, 209.0851.

**4-(4-Methylamino-phenylethynyl)-phenol (9b).** Compound **9b** was prepared using similar procedure as for **12a**: yield 88%. $^1$H NMR (200 MHz, $CDCl_3$, $\delta$ ppm): 2.74 (s, 3H), 6.53 (d, *J* = 8.7 Hz, 2H), 6.74 (d, *J* = 8.7 Hz, 2H), 7.18−7.30 (m, 4H). HRMS calcd for $C_{15}H_{13}NO$ ($M^+$), 223.0997; found, 223.0996.

**4-(4-Methoxy-phenylethynyl)-phenol (9c).** Compound **9c** was prepared according to method A: yield 52%. $^1$H NMR (200 MHz, $CDCl_3$, $\delta$ ppm): 3.82 (s, 3H), 6.75−6.90 (m, 4H), 7.36−7.47 (m. 4H). HRMS calcd for $C_{15}H_{12}O_2$ ($M^+$), 224.0837; found, 224.0841.

**4-(4-Amino-phenylethynyl)-phenylamine (9d).** Compound **9d** was prepared according to method A: yield 68%. $^1$H NMR (200 MHz, $CDCl_3$, $\delta$ ppm): 6.58−6.64 (m, 4H), 7.26−7.33 (m, 4H). HRMS calcd for $C_{14}H_{12}N_2$ ($M^+$), 208.1000; found, 208.1011.

**4-(4-Methoxy-phenylethynyl)-phenylamine (9e).** Compound **9e** was prepared according to method A: yield 50%. $^1$H NMR (200 MHz, $CD_3OD$, $\delta$ ppm): 3.80 (s, 3H), 6.62 (d, *J* = 8.7 Hz, 2H), 6.73 (d, *J* = 8.8 Hz, 2H), 7.18 (d, *J* = 8.7 Hz, 2H), 7.24 (d, *J* = 8.8 Hz, 2H). HRMS calcd for $C_{15}H_{13}NO$ ($M^+$), 223.0997; found, 223.0991.

**4-(4-(2-(2-Fluoro-ethoxy)-ethoxy)-phenylethynyl)-phenylamine (11a).** Compound **11a** was prepared according to method A: yield 68%. $^1$H NMR (200 MHz, $CDCl_3$, $\delta$ ppm): 3.72−3.91 (m, 4H), 4.15 (t, *J* = 4.4 Hz, 2H), 4.59 (dt, *J* = 47.6, 4.2 Hz, 2H), 6.62 (d, *J* = 8.6 Hz, 2H), 6.87 (d, *J* = 8.8 Hz, 2H), 7.31 (d, *J* =

**Scheme 1**[a]

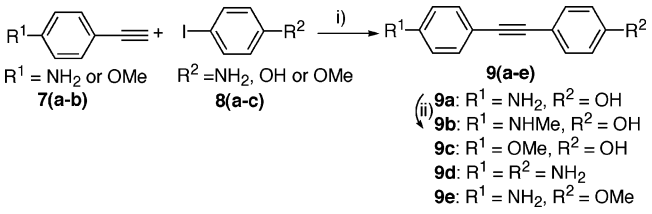


[a] Reagents and conditions: (i) $PdCl_2(PPh_3)_2$/CuI, 0.5 M $NH_4OH$, THF, rt, 4 h; (ii) (a) NaOMe, $(CH_2O)_n$, MeOH, reflux, 2 h; (b) $NaBH_4$, reflux, 1 h.

8.6 Hz, 2H), 7.41 (d, 8.8 Hz, 2H). HRMS calcd for $C_{18}H_{18}FNO_2$ ($M^+$), 299.1322; found, 299.1313.

**4-(4-(2-(2-(2-Fluoro-ethoxy)-ethoxy)-ethoxy)-phenylethynyl)-phenylamine (11b).** Compound **11b** was prepared according to method A: yield 72%. $^1$H NMR (200 MHz, $CDCl_3$, $\delta$ ppm): 3.65−3.86 (m, 8H), 4.09−4.16 (m, 2H), 4.56 (dt, $J$ = 49.7, 3.5 Hz, 2H), 6.62 (d, $J$ = 8.6 Hz, 2H), 6.86 (d, $J$ = 8.8 Hz, 2H), 7.30 (d, $J$ = 8.6 Hz, 2H), 7.41 (d, $J$ = 8.8.Hz, 2H). HRMS calcd for $C_{20}H_{22}FNO_3$ ($M^+$), 343.1584; found, 343.1572.

**(4-(4-(2-(2-Fluoro-ethoxy)-ethoxy)-phenylethynyl)-phenyl)-methylamine (12a).** Under argon atmosphere, sodium methoxide (33 mg, 0.60 mmol) was added to a solution of compound **11a** (40 mg, 0.12 mmol) in methanol (8 mL), followed by paraformaldehyde (18 mg, 0.60 mmol). The solution was heated to reflux for 2 h. After cooling the mixture to 0 °C, sodium borohydride (23 mg, 0.60 mmol) was added in portions, and the mixture was refluxed further for 1 h. The mixture was then poured into crushed ice and extracted with ethyl acetate (3 × 10 mL). The combined ethyl acetate layers were dried over $MgSO_4$, concentrated, and purified using preparative thin layer chromatography to afford **12a** in 88% yield. $^1$H NMR (200 MHz, $CDCl_3$, $\delta$ ppm): 2.85 (s, 3H), 3.72−3.76 (m, 1H), 3.87−3.91 (m, 3H), 4.14 (t, $J$ = 4.4 Hz, 2H), 4.59 (dt, $J$ = 47.6, 4.2 Hz, 2H), 6.54 (d, $J$ = 8.7 Hz, 2H), 6.87 (d, $J$ = 8.9 Hz, 2H), 7.34 (d, $J$ = 8.7 Hz, 2H), 7.42 (d, $J$ = 8.9 Hz, 2H). HRMS calcd for $C_{19}H_{20}FNO_2$ ($M^+$), 313.1478; found, 313.1467.

**(4-(4-(2-(2-(2-Fluoro-ethoxy)-ethoxy)-ethoxy)-phenylethynyl)-phenyl)-methylamine (12b).** Compound **12b** was prepared in 90% yield from **11b** following the same procedure as described for **12a**. $^1$H NMR (200 MHz, $CDCl_3$, $\delta$ ppm): 2.84 (s, 3H), 3.66−3.88 (m, 8H), 4.11 (t, $J$ = 4.4 Hz, 2H), 4.56 (dt, $J$ = 47.6, 4.2 Hz, 2H), 6.54 (d, $J$ = 8.7 Hz, 2H), 6.86 (d, $J$ = 8.8 Hz, 2H), 7.34 (d, $J$ = 8.7 Hz, 2H), 7.41 (d, $J$ = 8.8 Hz, 2H). HRMS calcd for $C_{21}H_{24}FNO_3$ ($M^+$), 357.1740; found, 357.1724.

**(4-(4-(2-(2-Fluoro-ethoxy)-ethoxy)-phenylethynyl)-phenyl)-dimethylamine (14a).** Compound **14a** was prepared according to method B: yield 80%. $^1$H NMR (200 MHz, $CDCl_3$, $\delta$ ppm): 2.97 (s, 6H), 3.74 (t, $J$ = 4.2 Hz, 1H), 3.87−3.91 (m, 3H), 4.13−4.17 (m, 2H), 4.59 (dt, $J$ = 47.6, 4.2 Hz, 2H), 6.65 (d, $J$ = 8.8 Hz, 2H), 6.87 (d, $J$ = 8.7 Hz, 2H), 7.35−7.44 (m, 4H). HRMS calcd for $C_{20}H_{22}FNO_2$ ($M^+$), 327.1635; found, 327.1635.

**(4-(4-(2-(2-(2-Fluoro-ethoxy)-ethoxy]-ethoxy)-phenylethynyl)-phenyl]-dimethylamine (14b).** Compound **14b** was prepared according to method B: yield 84%. $^1$H NMR (200 MHz, $CDCl_3$, $\delta$ ppm): 2.97 (s, 6H), 3.65−3.68 (m, 8H), 4.14 (t, $J$ = 4.8 Hz, 2H) 4.56 (dt, $J$ = 48.5, 3.2 Hz, 2H), 6.65 (d, $J$ = 8.8 Hz, 2H), 6.86 (d, $J$ = 8.8 Hz, 2H), 7.35−7.43 (m, 4H). HRMS calcd for $C_{22}H_{26}FNO_3$ ($M^+$), 371.1897; found, 371.1882.

**(4-(2-(2-(2-Fluoro-ethoxy)-ethoxy)-ethoxy)-phenylethynyl)-trimethylsilane (15).** To a solution of **10b** (354 mg, 1 mmol) and TMSA (0.207 mL, 1.5 mmol) in triethylamine (10 mL) was added $PdCl_2(PPh_3)_2$ (5 mol %) and CuI (3 mol %) at 0 °C under an argon atmosphere. The mixture was stirred at 0 °C for 2 h and then at room temperature overnight. After evaporation of the solvent, the crude residue was purified using silica gel column (20% ethyl acetate in hexanes) to afford **15** in 78% yield. $^1$H NMR (200 MHz, $CDCl_3$, $\delta$ ppm): 0.22 (s, 9H), 3.66−3.86 (m, 8H), 4.12 (t, $J$ = 4.4 Hz, 2H), 4.54 (dt, $J$ = 47.6, 4.2 Hz, 2H), 6.82 (d, $J$ = 8.8 Hz, 2H), 7.38 (d, $J$ = 8.8 Hz, 2H).

**1-Ethynyl-4-(2-(2-(2-fluoro-ethoxy)-ethoxy)-ethoxy)-benzene (16).** To a solution of **15** (162 mg, 0.5 mmol) in methanol (8 mL) was added KOH (66 mg, 1 mmol) in methanol (4 mL). The mixture was stirred at room temperature for 10 h. The residue, after the evaporation of the volatiles, was purified using silica gel column chromatography (20% ethyl acetate in hexanes) to afford **16** in 82% yield. $^1$H NMR (200 MHz, $CDCl_3$, $\delta$ ppm): 2.98 (s, 1H), 3.64−3.88 (m, 8H), 4.05−4.13 (m, 2H), 4.55 (dt, $J$ = 47.6, 4.2 Hz, 2H), 6.85 (d, $J$ = 8.8 Hz, 2H), 7.41(d, $J$ = 8.8 Hz, 2H).

**4-(4-(2-(2-(2-Fluoro-ethoxy)-ethoxy)-ethoxy)-phenylethynyl)-phenol (17).** Compound **17** was prepared according to method A: yield 58%. $^1$H NMR (200 MHz, $CDCl_3$, $\delta$ ppm): 3.66−3.88 (m, 8H), 4.11 (t, $J$ = 4.4 Hz, 2H), 4.56 (dt, $J$ = 47.6, 4.1 Hz, 2H), 6.78 (d, $J$ = 8.6 Hz, 2H), 6.83 (d, $J$ = 8.8 Hz, 2H), 7.36 (d, $J$ = 8.6 Hz, 2H), 7.42 (d, $J$ = 8.8 Hz, 2H). HRMS calcd for $C_{20}H_{21}FO_4$ ($M^+$), 344.1424; found, 344.1426.

**2-(2-(4-(4-Amino-phenylethynyl)-phenoxy)-ethoxy)-ethanol (19a).** Compound **19a** was prepared according to method A: yield 52%. $^1$H NMR (200 MHz, $CDCl_3$, $\delta$ ppm): 3.64−3.88 (m, 6H), 4.09−4.16 (m, 2H), 6.62 (d, $J$ = 8.4 Hz, 2H), 6.86 (d, $J$ = 8.7 Hz, 2H), 7.30 (d, $J$ = 8.4 Hz, 2H), 7.41 (d, $J$ = 8.7 Hz, 2H).

**2-(2-(2-(4-(4-Amino-phenylethynyl)-phenoxy)-ethoxy)-ethoxy)-ethanol (19b).** Compound **19b** was prepared according to method A: yield 64%. $^1$H NMR (200 MHz, $CDCl_3$, $\delta$ ppm): 3.58−3.75 (m, 8H), 3.83−3.88 (m, 2H), 4.09−4.15 (m, 2H), 6.62 (d, $J$ = 8.6 Hz, 2H), 6.86 (d, $J$ = 8.8 Hz, 2H), 7.30 (d, $J$ = 8.6 Hz, 2H), 7.41 (d, $J$ = 8.8 Hz, 2H). HRMS calcd for $C_{20}H_{23}NO_4$ ($M^+$), 341.1627; found, 341.1621.

**4-(4-(2-(2-(*tert*-Butyl-dimethyl-silanyloxy)-ethoxy)-ethoxy)-phenylethynyl)-phenylamine (19c).** Compound **19c** was prepared according to method A: yield 62%. $^1$H NMR (200 MHz, $CDCl_3$, $\delta$ ppm): 0.07 (s, 6H), 0.89 (s, 9H), 3.59−3.63 (m, 2H), 3.76−3.88 (m, 4H), 4.09−4.14 (m, 2H), 6.62 (d, $J$ = 8.6 Hz, 2H), 6.86 (d, $J$ = 8.8 Hz, 2H), 7.31 (d, $J$ = 8.6 Hz, 2H), 7.41 (d, $J$ = 8.8 Hz, 2H).

**4-(4-(2-(2-(2-(*tert*-Butyl-dimethyl-silanyloxy)-ethoxy)-ethoxy)-ethoxy)-phenylethynyl)-phenylamine (19d).** Compound **19d** was prepared according to method A: yield 66%. $^1$H NMR (200 MHz, $CDCl_3$, $\delta$ ppm): $^1$H NMR (200 MHz, $CDCl_3$, $\delta$) 0.61 (s, 6H), 0.89 (s, 9H), 3.53−3.88 (m, 10H), 4.10−4.15 (m, 2H), 6.61 (d, $J$ = 8.6 Hz, 2H), 6.86 (d, $J$ = 8.8 Hz, 2H), 7.31 (d, $J$ = 8.6 Hz, 2H), 7.40 (d, $J$ = 8.8 Hz, 2H).

**2-(2-(4-(4-Methylamino-phenylethynyl)-phenoxy)-ethoxy)-ethanol (20a).** Compound **20a** was prepared in 85% yield from **19a** following the same procedure as described for **12a**. $^1$H NMR (200 MHz, $CDCl_3$, $\delta$ ppm):2.84 (s, 3H), 3.64−3.88 (m, 6H), 4.11−4.16 (m, 2H), 6.54 (d, $J$ = 8.6 Hz, 2H), 6.87 (d, $J$ = 8.7 Hz, 2H), 7.34 (d, $J$ = 8.6 Hz, 2H), 7.42 (d, $J$ = 8.7 Hz, 2H). HRMS calcd for $C_{19}H_{21}NO_3$ ($M^+$), 311.1521; found, 311.1521.

**2-(2-(2-(4-(4-Methylamino-phenylethynyl)-phenoxy)-ethoxy)-ethoxy)-ethanol (20b).** Compound **20b** was prepared in 92% yield from **19b** following the same procedure as described for **12a**. $^1$H NMR (200 MHz, $CDCl_3$, $\delta$ ppm): 2.84 (s, 3H), 3.59−3.75 (m, 8H), 3.83−3.88 (m, 2H), 4.09−4.16 (m, 2H), 6.55 (d, $J$ = 8.6 Hz, 2H), 6.86 (d, $J$ = 8.8 Hz, 2H), 7.33 (d, $J$ = 8.6 Hz, 2H), 7.42 (d, $J$ = 8.8 Hz, 2H). HRMS calcd for $C_{21}H_{25}NO_4$ ($M^+$), 355.1784; found, 355.1789.

**(4-(4-(2-(2-(*tert*-Butyl-dimethyl-silanyloxy)-ethoxy)-ethoxy)-phenylethynyl)-phenyl)-methylamine (20c).** Compound **20c** was prepared in 90% yield from **19c** following the same procedure as described for **12a**. $^1$H NMR (200 MHz, $CDCl_3$, $\delta$ ppm): 0.07 (s, 6H), 0.89 (s, 9H), 2.85 (s, 3H), 3.60−3.63 (m, 2H), 3.76−3.88 (m, 4H), 4.09−4.14 (m, 2H), 6.54 (d, $J$ = 8.7 Hz, 2H), 6.86 (d, $J$ = 8.9 Hz, 2H), 7.34 (d, $J$ = 8.7 Hz, 2H), 7.41 (d, $J$ = 8.9 Hz, 2H).

**(4-(4-(2-(2-(2-(*tert*-Butyl-dimethyl-silanyloxy)-ethoxy)-ethoxy)-ethoxy)-phenylethynyl)-phenyl)-methylamine (20d).** Compound **20d** was prepared in 94% yield from **19d** following the same procedure as described for **12a**. $^1$H NMR (200 MHz, $CDCl_3$, $\delta$ ppm): 0.66 (s, 6H), 0.89 (s, 9H), 2.83 (s, 3H), 3.56 (t, 5.3 Hz, 2H), 3.69−3.87 (m, 8H), 4.10−4.14 (m, 2H), 6.53 (d, $J$ = 8.6 Hz,

**Scheme 2**[a]

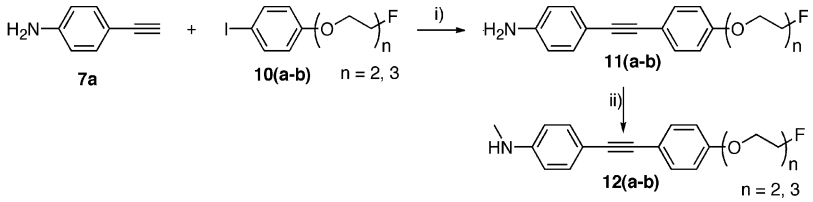


[a] Reagents and conditions: (i) $PdCl_2(PPh_3)_2$/CuI, 0.5 M $NH_4OH$, THF, rt, 4 h; (ii) (a) NaOMe, $(CH_2O)_n$, MeOH, reflux, 2 h; (b) $NaBH_4$, reflux, 1 h.

**Scheme 3**[a]

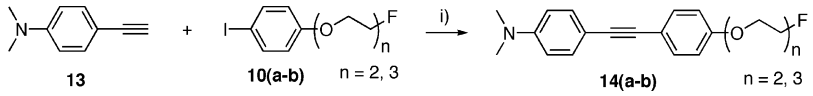


[a] Reagents and conditions: (i) $PdCl_2(PPh_3)_2$/CuI, TEA, THF, Ar + $H_2$, 60 °C, 16 h.

**Scheme 4**[a]

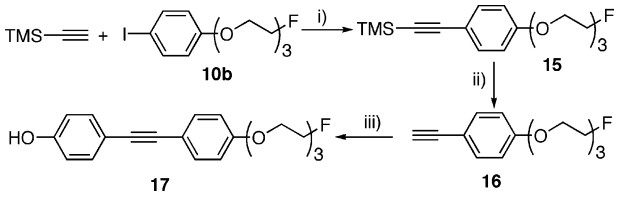


[a] Reagents and conditions: (i) $PdCl_2(PPh_3)_2$/CuI, TEA, 0 °C−rt, 16 h; (ii) KOH, MeOH, rt, 16 h; (iii) *p*-iodophenol, $PdCl_2(PPh_3)_2$/CuI, 0.5 M $NH_4OH$, THF, rt, 4 h.

2H), 6.85 (d, $J$ = 8.6 Hz, 2H), 7.33 (d, $J$ = 8.6 Hz, 2H), 7.41 (d, $J$ = 8.6 Hz, 2H).

**(4-(4-(2-(2-(*tert*-Butyl-dimethyl-silanyloxy)-ethoxy)-ethoxy)-phenylethynyl)-phenyl)-methyl-carbamic Acid *tert*-Butyl Ester (21c).** A solution of **20c** (106 mg, 0.25 mmol), di-*tert*-butyl dicarbonate (110 mg, 0.50 mmol), and catalytic DMAP (10 mg) was refluxed in anhydrous THF (4 mL) for 16 h. Another portion of di-*tert*-butyl dicarbonate (55 mg, 0.25 mmol) was then added, and the mixture was refluxed again for 10 h. The volatiles were then removed under reduced pressure, and the resulting residue was purified by silica gel column chromatography (20% EtOAc in hexanes) to afford **12c** in 52% yield. $^1$H NMR (200 MHz, $CDCl_3$, $\delta$ ppm): 0.73 (s, 6H), 0.89 (s, 9H), 1.45 (s, 9H), 3.26 (s, 3H), 3.60−3.65 (m, 2H), 3.77−3.89 (m, 4H), 4.10−4.15 (m, 2H), 6.88 (d, $J$ = 8.7 Hz, 2H), 7.20 (d, $J$ = 8.5 Hz, 2H), 7.42−7.47 (m, 4H).

**(4-(4-(2-(2-(2-(*tert*-Butyl-dimethyl-silanyloxy)-ethoxy)-ethoxy)-ethoxy)-phenylethynyl)-phenyl)-methyl-carbamic Acid *tert*-Butyl Ester (21d).** Compound **21d** was prepared in 58% yield from **20d** following the same procedure as described for **21c**. $^1$H NMR (200 MHz, $CDCl_3$, $\delta$ ppm): 0.63 (s, 6H), 0.89 (s, 9H), 1.45 (s, 9H), 3.26 (s, 3H), 3.56 (t, 5.4 Hz, 2H), 3.64−3.88 (m, 8H), 4.11−4.16 (m, 2H), 6.88 (d, $J$ = 8.7 Hz, 2H), 7.20 (d, $J$ = 8.5 Hz, 2H), 7.41−7.46 (m, 4H).

**Methanesulfonic Acid 2-(2-(4-(4-(*tert*-Butoxycarbonyl-methyl-amino)-phenylethynyl)-phenoxy)-ethoxy)-ethyl Ester (22c).** Compound **21c** (36 mg, 0.07 mmol) was dissolved in 1 mL dry THF, and the solution was cooled to 0 °C. Tetrabutylammonium bromide (0.17 mL, 1 M solution in THF) was then added, and the mixture was stirred at room temperature for 2 h and after which was quenched with ice. The mixture was then extracted with EtOAc (3 × 8 mL), and the combined organic layer was dried ($MgSO_4$) and concentrated. The crude residue was dissolved in dry dichloromethane (4 mL) and cooled to 0 °C. Triethyl amine (40 $\mu$L, 0.28 mmol) and MsCl (17 $\mu$L, 0.21 mmol) were added to the reaction mixture and stirred at room temperature for 3 h. After quenching with cold water, the reaction mixture was extracted with DCM (3 × 5 mL). The combined organic layer was dried, concentrated, and purified by PTLC (60% EtOAc in hexanes) to afford **22c** in 80% yield over two steps. $^1$H NMR (200 MHz, $CDCl_3$, $\delta$ ppm): 1.45 (s, 9H), 3.04 (s, 3H), 3.26 (s, 3H), 3.81−3.90 (m, 4H), 4.12−4.16 (m, 2H), 4.37−4.42 (m, 2H), 6.86 (d, $J$ = 8.7 Hz, 2H), 7.21 (d, $J$ = 8.5 Hz, 2H), 7.42−7.47 (m, 4H).

**Methanesulfonic Acid 2-(2-(2-(4-(4-(*tert*-Butoxycarbonyl-methyl-amino)-phenylethynyl)-phenoxy)-ethoxy)-ethoxy)-ethyl Ester (22d).** Compound **22d** was prepared in 94% yield from **21d** following the same procedure as described for **22c**. $^1$H NMR (200 MHz, $CDCl_3$, $\delta$ ppm): 1.45 (s, 9H), 3.04 (s, 3H), 3.26 (s, 3H), 3.68−3.87 (m, 8H), 4.11−4.16 (m, 2H), 4.35−4.39 (m, 2H), 6.87 (d, $J$ = 8.6 Hz, 2H), 7.20 (d, $J$ = 8.4 Hz, 2H), 7.42−7.47 (m, 4H).

**2-(2-(4-(4-Dimethylamino-phenylethynyl)-phenoxy)-ethoxy)-ethanol (23a).** Compound **23a** was prepared according to method B: yield 80%. $^1$H NMR (200 MHz, $CDCl_3$, $\delta$ ppm): 2.97 (s, 6H), 3.65−3.89 (m, 6H), 4.10−4.16 (m, 2H), 6.65 (d, $J$ = 8.8 Hz, 2H), 6.86 (d, $J$ = 8.8 Hz, 2H), 7.34−7.44 (m, 4H). HRMS calcd for $C_{20}H_{23}NO_3$ ($M^+$), 325.1678; found, 325.1675.

**2-(2-(2-(4-(4-Dimethylamino-phenylethynyl)-phenoxy)-ethoxy)-ethoxy)-ethanol (23b).** Compound **23b** was prepared according to method B: yield 82%. $^1$H NMR (200 MHz, $CDCl_3$, $\delta$ ppm): 2.97 (s, 6H), 3.47−3.65 (m, 8H), 3.79−3.84 (m, 2H), 4.10−4.17 (m, 2H), 6.70 (d, $J$ = 8.9 Hz, 2H), 6.94 (d, $J$ = 8.8 Hz, 2H), 7.32 (d, $J$ = 8.9 Hz, 2H), 7.39 (d, $J$ = 8.8 Hz, 2H). HRMS calcd for $C_{22}H_{27}NO_4$ ($M^+$), 369.1940; found, 369.1934.

**Methanesulfonic Acid 2-(2-(4-(4-Dimethylamino-phenylethynyl)-phenoxy)-ethoxy)-ethyl Ester (24a).** A solution of **23a** (20 mg, 0.06 mmol) in dry DCM was cooled to 0 °C, and TEA (22 $\mu$L, 0.15 mmol) was added followed by MsCl (6 $\mu$L, 0.07 mmol). The reaction mixture was stirred initially at 0 °C and then at room temperature for 2 h. After quenching the reaction with cold water, the organic layer was separated. The aqueous layer was further extracted with DCM (2 × 5 mL). The combined organic extracts were dried ($MgSO_4$) and concentrated, and the residue was purified by PTLC (50% EtOAc in hexanes) to afford **24a** in 78% yield. $^1$H NMR (200 MHz, $CDCl_3$, $\delta$ ppm): 2.97 (s, 6H), 3.08 (s, 3H), 3.65−3.75 (m, 4H), 3.82−3.89 (m, 2H), 4.07−4.16 (m, 2H), 6.65 (d, $J$ = 8.9 Hz, 2H), 6.85 (d, $J$ = 8.8 Hz, 2H), 7.34−7.44 (m, 4H).

**Methanesulfonic Acid 2-(2-(2-(4-(4-Dimethylamino-phenylethynyl)-phenoxy)-ethoxy)-ethoxy)-ethyl Ester (24b).** Compound **24b** was prepared in 84% yield from **23b** following the same procedure as described for **24a**. $^1$H NMR (200 MHz, $CDCl_3$, $\delta$ ppm): 2.97 (s, 6H), 3.09 (s, 3H), 3.62−3.84 (m, 8H), 4.12−4.18 (m, 2H), 4.32−4.37 (m, 2H), 6.71 (d, $J$ = 8.9 Hz, 2H), 6.95 (d, $J$ = 8.8 Hz, 2H), 7.32 (d, $J$ = 8.9 Hz, 2H), 7.40 (d, $J$ = 8.8 Hz, 2H).

**(4-(4-(2-(2-[$^{18}$F]Fluoro-ethoxy)-ethoxy)-phenylethynyl)-phenyl)-methylamine, [$^{18}$F]12a.** [$^{18}$F]Fluoride was produced by the JSW typeBC3015 cyclotron using $^{18}O(p,n)^{18}F$ reaction and passed through a Sep-Pak Light QMA cartridge (waters) as an aqueous solution in [$^{18}$O]-enriched water. The cartridge was dried by airflow, and the $^{18}$F activity was eluted with 2 mL of Kryptofix 222 (K222)/$K_2CO_3$ solution (13.2 mg of K222 and 3.0 mg of $K_2CO_3$ in $CH_3CN/H_2O$ 1.12/0.18). The solvent was removed at 120 °C under an argon stream. The residue was azeotropically dried with 1 mL of anhydrous $CH_3CN$ twice at 120 °C under a nitrogen stream. A

**Scheme 5**[a]

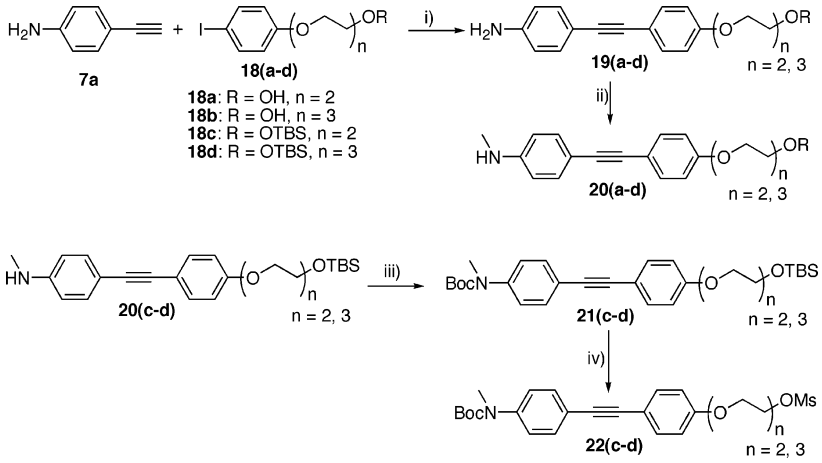


[a] Reagents and conditions: (i) $PdCl_2(PPh_3)_2$/CuI, 0.5 M $NH_4OH$, THF, rt, 4 h; (ii) (a) NaOMe, $(CH_2O)_n$, MeOH, reflux, 2 h; (b) $NaBH_4$, reflux, 1 h; (iii) $(Boc)_2O$, DMAP, THF, relux, 24 h; (iv) (a) TBAF (1 M in THF), 0 °C−rt, 2 h; (b) MsCl, TEA, DCM, 0 °C−rt, 3 h.

**Scheme 6**[a]

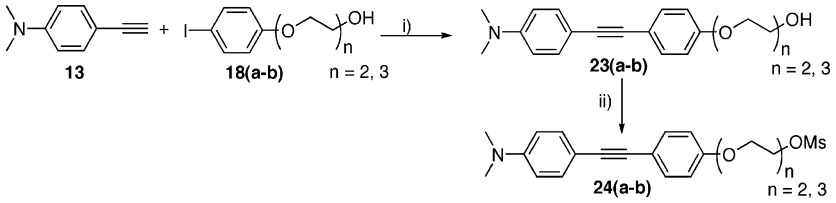


[a] Reagents and conditions: (i) $PdCl_2(PPh_3)_2$/CuI, TEA, THF, Ar + $H_2$, 60 °C, 16 h; (ii) MsCl, TEA, DCM, 0 °C−rt, 2 h.

**Scheme 7**[a]

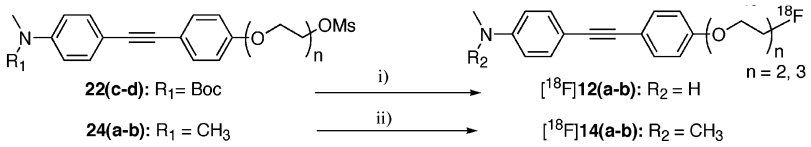


[a] Reagents and conditions: (i) (1)$^{18}F^-$/K222, DMSO; (2) microwave, 100 W, DMSO, (ii) $^{18}F^-$/K222, DMSO.

solution of mesylate precursor **22c** (1 mg) in DMSO (0.5 mL) was added to the reaction vessel containing the dried $^{18}F$ activities. The mixture was heated at 120 °C for 4 min. To remove the Boc protecting group, the mixture was further irradiated with microwave at 100 W (Resonance Instruments Model 521) at 150 °C for 3 min. Water (5 mL) was added, and the mixture was passed through a preconditioned OASIS HLB cartridge (3 $cm^3$; Waters). The cartridge was washed with 10 mL of water, and labeled compound was eluted with 2 mL of $CH_3CN$. Eluted compound was purified by HPLC. [Phenonemex Gemini C18 semi-prep column (10 × 250 mm, 5 $\mu$m), $CH_3CN$/water 7/3, flow rate 3 mL/min, rt = 9.6 min.] The entire preparation procedure took approximately 90 min. The radiochemical yield was 20% (decay corrected). The radiochemical purity and specific activity were determined by analytical HPLC. [Phenomenex Gemini C18 analytical column (4.6 × 250 mm, 5 $\mu$m), $CH_3CN$/ammonium formate buffer (1 mM) 8/2; Flow rate 1 mL/min; rt = 5.3 min.] The radiochemical purity was >99%. Specific activity was estimated by comparing UV peak intensity of purified [$^{18}F$]-labeled compound with reference nonradioactive compound of known concentration. The specific activity was in the range of 600−1300 mCi/$\mu$mol after the preparation.

**(4-(4-(2-(2-(2-[$^{18}$F]Fluoro-ethoxy)-ethoxy)-ethoxy)-phenylethynyl)-phenyl)-methylamine (12b), [$^{18}$F]12b.** The above-described procedure for [$^{18}F$]**12a** was applied for precursor **22d**. The final compound was purified and analyzed by HPLC (same conditions). Rt (semi-prep) = 9.3 min, (analytical) = 5.2 min. The preparation took approximately 90 min. The radiochemical yield was 20% (decay corrected). The radiochemical purity was >99%. Specific activity was approximately 600 mCi/$\mu$mol after the preparation.

**(4-(4-(2-(2-[$^{18}$F]Fluoro-ethoxy)-ethoxy)-phenylethynyl)-phenyl)-dimethylamine (14a), [$^{18}$F]14a.** The procedure for [$^{18}F$]**12a** was followed for precursor **2a** up to the initial reaction of **2a** with $^{18}K$/K222 by heating. After the initial heating was complete, water (5 mL) was added and the mixture was passed through a preconditioned OASIS HLB cartridge (3 $cm^3$; Waters). The cartridge was washed with 10 mL of water, and the labeled compound was eluted with 2 mL of $CH_3CN$. The eluted compound was purified and analyzed by HPLC (same condition). Rt (semi-prep) = 13,8 min (4 mL/min), (analytical) = 7.6 min. The preparation took approximately 60 min. The radiochemical yield was 30% (decay corrected). The radiochemical purity was >99%. Specific activity was in the range of 1100−4600 mCi/$\mu$mol after the preparation.

**(4-(4-(2-(2-(2-[$^{18}$F]Fluoro-ethoxy)-ethoxy)-ethoxy)-phenylethynyl)-phenyl)-dimethylamine (14b), [$^{18}$F]14b.** Same procedure for [$^{18}F$]**14a** was applied for precursor **12b**. The final compound was purified and analyzed by HPLC. Rt (semi-prep column) = 14.0 min (4 mL/min), (analytical) = 7.3 min. The preparation took approximately 60 min. The radiochemical yield was 30% (decay corrected), and the radiochemical purity was >97%. Specific activity was approximately 980−4000 mCi/$\mu$mol after the preparation.

**Preparation of Brain Tissue Homogenates.** AD postmortem brain tissues were obtained from University of Washington Alzheimer's Disease Research Center, and neuropathological diagnosis was confirmed by current criteria (NIA-Reagan Institute Consensus Group, 1997). Homogenates were then prepared from dissected gray matters from four pooled AD patients in phosphate buffered saline (PBS, pH 7.4) at the concentration of approximately 100 mg wet tissue/mL (motor-driven glass homogenizer with setting of 6 for

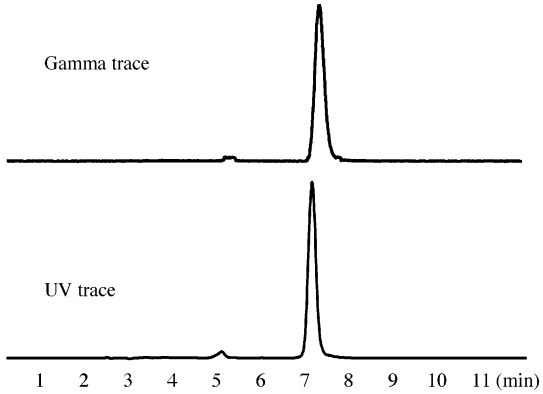


**Figure 2.** HPLC profiles of [$^{18}$F]**14b** (top) and **14b** (bottom). HPLC condition: Agilent 1100 series; Gemini C-18 column $CH_3CN$/ammonium formate (10 mM) 8/2 1 mL/min, 254 nm, $t_R$ = (UV) 7.04 min, (_) 7.29 min. The slight difference in retention time between the radioactive peak and the UV peak is due to the configuration of detector system).

30 s). The homogenates were aliquoted into 1 mL portions and stored at −70 °C up to 2 years without loss of binding signal.

**Binding Studies.** [$^{125}$I]IMPY, **4**, with 2200 Ci/mmol specific activity and greater than 95% radiochemical purity was prepared using the standard iododestannylation reaction and purified by a simplified C-4 mini column as described previously.[32] Competition binding assays were carried out in 12 × 75 mm borosilicate glass tubes. The reaction mixture contained 50 $\mu$L of pooled AD brain homogenates (20−50 $\mu$g), 50 $\mu$L of [$^{125}$I]IMPY, **4**, (0.04−0.06 nM diluted in PBS), and 50 $\mu$L of inhibitors ($10^{-5}$−$10^{-10}$ M diluted serially in PBS containing 0.1% bovine serum albumin) in a final volume of 1 mL. Nonspecific binding was defined in the presence of 600 nM IMPY, **4**, in the same assay tubes. The mixture was incubated at 37 °C for 2 h, and the bound and the free radioactivity were separated by vacuum filtration through Whatman GF/B filters using a Brandel M-24R cell harvester followed by 2 × 3 mL washes of PBS at room temperature. Filters containing the bound I-125 ligand were counted in a gamma counter (Packard 5000) with 70% counting efficiency. Under the assay conditions, the non-specifically bound fraction was less than 15% of the total radioactivity. Inhibition experiments were repeated three times, and the results were subjected to nonlinear regression analysis using equilibrium binding data analysis, which $K_i$ values were calculated.

Similarly, specific binding of [$^{18}$F]**12b** (0.001−0.4 nM) to homogenates, prepared from gray matters of four pooled AD patients, were carried out as described above. Nonspecific binding was determined in the presence of 800 nM of nonradioactive **12b**.

**Film Autoradiography.** To compare different probes using similar sections of human brain tissues, a human brain macro-array from six confirmed AD cases and one control subject was assembled. The presence and localization of plaques on the sections were confirmed with immunohistochemistry stained with monoclonal A$\beta$ antibody 4G8 (Signet Lab. Inc. Dedham, MA). The sections were incubated with [$^{18}$F]tracers (300 000−600 000 cpm/200 $\mu$L) for 1 h at room temperature. The sections were then dipped in saturated $Li_2CO_3$ in 40% EtOH (2 min wash × 2) and washed with 40% EtOH (2 min wash × 1), followed by rinsing with water for 30 s. After drying, the $^{18}$F-labeled sections were exposed to Kodak Biomax MR film overnight.

**Organ Distribution in Normal Mice.** While under isoflurane anesthesia, 0.15 mL of a 0.1% bovine serum albumin solution containing [$^{18}$F]tracers (5−10 $\mu$Ci) was injected directly into the tail vein of ICR mice (22−25 g, male). The mice ($n$ = 3 for each time point) were sacrificed by cervical dislocation at designated time points postinjection. The organs of interest were removed and weighed, and the radioactivity was counted with an automatic gamma counter. The percentage dose per organ was calculated by a comparison of the tissue counts to suitably diluted aliquots of the injected material. Total activities of blood were calculated under the assumption that they were 7% of the total body weight. The % dose/g of samples was calculated by comparing the sample counts with the count of the diluted initial dose.

**Partition Coefficient.** Partition coefficients were measured by mixing the [$^{18}$F]tracer with 3 g each of 1-octanol and buffer (0.1 M phosphate, pH 7.4) in a test tube. The test tube was vortexed for 3 min at room temperature, followed by centrifugation for 5 min. Two weighed samples (0.5 g each) from the 1-octanol and buffer layers were counted in a well counter. The partition coefficient was determined by calculating the ratio of cpm/g of 1-octanol to that of buffer. Samples from the 1-octanol layer were repartitioned until consistent partitions of coefficient values were obtained. The measurement was done in triplicate and repeated three times.

## Results and Discussion

**Chemistry and Radiochemistry.** The synthesis of the diphenylacetylene core structures was easily achieved as given in Scheme 1. The key step in the synthesis of these compounds was the Pd(0)/Cu(I)-catalyzed (Sonogashira) coupling of the suitably substituted iodobenzenes **8**(**a**−**c**) with appropriately functionalized phenyl acetylenes **7**(**a**,**b**). Dimerization of acetylene was a side reaction under these conditions, and dimers are typically formed in 10−20% yield.

The coupling of amino-substituted phenylacetylene **7a** with *para*-F-PEG iodobenzenes **10**(**a**,**b**) in THF using 0.5 M $NH_4$-OH (Method A,[33] see Experimental Section) as base afforded compounds **11**(**a**,**b**). Subsequent monomethylation of the $NH_2$ group in **11**(**a**,**b**) under standard conditions afforded monomethylated derivatives **12**(**a**,**b**; Scheme 2).

However, the coupling of *N*,*N*-dimethyl-substituted acetylene **13** with **10**(**a**,**b**) under similar conditions yielded appreciable amounts of dimer, the desired products were formed only in negligible amounts. To circumvent this, Sonogashira reaction was carried out under a reducing atmosphere.[34] Thus, under a gaseous mixture of hydrogen (10−50%) and argon, the reaction proceeded to afford the desired products **14**(**a**,**b**) in good yields (Scheme 3).

The synthesis of hydroxy-substituted derivative **17** started with the coupling of TMS acetylene with **10b**, which afforded the substituted phenylacetylene **16**. The subsequent removal of the TMS group in **15** followed by the coupling with *para*-iodophenol afforded the hydroxy derivative **17** (Scheme 4).

The synthesis of the precursors to the corresponding [$^{18}$F]-labeled compounds of *N*-monomethyl derivatives is depicted in Scheme 5. Compounds **19**(**a**−**d**), obtained by the coupling of acetylene **7a** with iodocompounds **18**(**a**−**d**), were monomethylated under the standard conditions to afford **20**(**a**−**d**). The amino groups in the TBS-protected compounds **20**(**c**,**d**) were then protected with Boc group. The subsequent removal of the TBS group followed by the mesylation of the resulting free hydroxy groups yielded precursors **22**(**c**,**d**). Compounds **22**(**c**,**d**) serve as the immediate precursors for the [$^{18}$F]-labeled **12**(**a**,**b**) (Scheme 5).

The precursors for [$^{18}$F]**14**(**a**,**b**) were obtained by the coupling of the phenylacetylene **13** with iodobenzene derivatives **18**(**a**,**b**) under reducing conditions (Scheme 6). The mesylation of the hydroxyl groups present in **23**(**a**,**b**) afforded the precursors **24**(**a**,**b**) (Scheme 7).

To obtain [$^{18}$F]**12a** and [$^{18}$F]**12b**, precursors (**22c** and **22d**, respectively) were reacted with [$^{18}$F]fluoride in the presence of Kryptofix 222 and potassium carbonate in DMSO at 100 °C for 4 min. The resulting [$^{18}$F]-labeled intermediates were irradiated with microwaves to deprotect the Boc group to provide the desired labeled compounds (Scheme 7). The crude product was purified by HPLC. The procedure took 90 min for

**Table 1.** Inhibition Constants (Ki, nM) of Compounds on [$^{125}$I]IMPY, 4, Binding to Amyloid Plaques in ad Brain Homogenates[a]

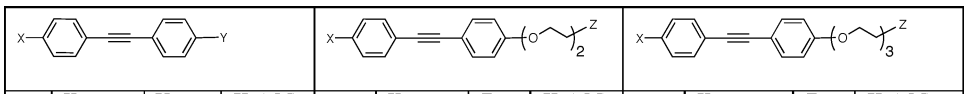

| | X | Y | Ki (nM) | | X | Z | Ki (nM) | | X | Z | Ki (nM) |
|---|---|---|---|---|---|---|---|---|---|---|---|
| **9** | H | H | 175 ± 35 | **11a** | $NH_2$ | F | 12 ± 2.9 | **11b** | $NH_2$ | F | 21.5 ± 6.5 |
| **9a** | $NH_2$ | OH | 106 ± 6 | **12a** | NHMe | F | 1.2 ± 0.2 | **12b** | NHMe | F | 1.9 ± 0.3 |
| **9b** | NHMe | OH | 1.5 ± 0.1 | **14a** | $NMe_2$ | F | 5.0 ± 1.0 | **14b** | $NMe_2$ | F | 2.9 ± 0.1 |
| **9c** | OMe | OH | 2.9 ± 0.3 | **20a** | NHMe | OH | 3.1 ± 0.6 | **17** | OH | F | 16.5 ± 3.5 |
| **9d** | $NH_2$ | $NH_2$ | 76 ± 15 | **23a** | $NMe_2$ | OH | 3.8 ± 0.8 | **19b** | $NH_2$ | OH | 67.5 ± 7.5 |
| **9e** | $NH_2$ | OMe | 2.9 ± 0.4 | | | | | **20b** | NHMe | OH | 4.5± 0.9 |
| | | | | | | | | **23b** | $NMe_2$ | OH | 3.4 ± 0.1 |

[a] Values are mean ± SEM of three independent experiments, each in duplicate.

**Table 2.** Biodistributions in ICR Mice after iv Injections of [$^{18}$F]Tracers[a]

| [$^{18}$F]**12a** (Log P = 3.48) | | | | |
|---|---|---|---|---|
| organ | 2 min | 30 min | 1 h | 2 h |
| blood | 7.89 ± 1.12 | 7.90 ± 0.93 | 10.3 ± 0.11 | 7.84 ± 0.33 |
| heart | 4.73 ± 1.06 | 2.84 ± 0.10 | 3.54 ± 0.20 | 2.60 ± 0.06 |
| muscle | 0.79 ± 0.22 | 1.26 ± 0.38 | 1.38 ± 0.25 | 1.26 ± 0.06 |
| lung | 6.57 ± 0.51 | 4.77 ± 0.45 | 6.01 ± 0.41 | 4.67 ± 0.31 |
| kidney | 5.55 ± 0.75 | 4.78 ± 0.66 | 6.17 ± 0.38 | 5.55 ± 0.68 |
| spleen | 3.74 ± 0.38 | 3.60 ± 0.61 | 3.78 ± 0.33 | 3.30 ± 0.04 |
| liver | 29.6 ± 1.36 | 18.3 ± 2.21 | 15.6 ± 2.43 | 11.7 ± 0.91 |
| skin | 0.94 ± 0.11 | 2.11 ± 0.36 | 2.55 ± 0.22 | 2.04 ± 0.12 |
| brain | 4.42 ± 0.88 | 1.03 ± 0.15 | 0.99 ± 0.09 | 0.82 ± 0.03 |
| bone | 1.54 ± 0.28 | 1.46 ± 0.21 | 1.92 ± 0.16 | 2.07 ± 0.14 |
| [$^{18}$F]**14a** (log P = 3.12) | | | | |
| organ | 2 min | 30 min | 1 h | 2 h |
| blood | 7.33 ± 0.43 | 6.13 ± 0.35 | 5.68 ± 0.75 | 5.17 ± 0.39 |
| heart | 10.5 ± 1.13 | 2.82 ± 1.13 | 2.48 ± 0.36 | 2.11 ± 0.13 |
| muscle | 0.91 ± 0.26 | 1.38 ± 0.15 | 1.21 ± 0.17 | 1.03 ± 0.09 |
| lung | 11.1 ± 0.99 | 4.66 ± 0.37 | 3.82 ± 0.55 | 3.38 ± 0.43 |
| kidney | 12.9 ± 1.51 | 4.75 ± 0.13 | 4.79 ± 0.82 | 4.16 ± 0.69 |
| spleen | 5.12 ± 0.95 | 2.94 ± 0.41 | 2.38 ± 0.43 | 2.31 ± 0.27 |
| liver | 19.3 ± 1.14 | 11.2 ± 0.49 | 9.99 ± 1.76 | 8.85 ± 0.72 |
| skin | 0.85 ± 0.15 | 2.23 ± 0.36 | 1.71 ± 0.70 | 1.67 ± 0.44 |
| brain | 5.41 ± 0.84 | 3.69 ± 0.25 | 2.06 ± 0.33 | 1.34 ± 0.12 |
| bone | 1.78 ± 0.15 | 1.41 ± 0.08 | 1.36 ± 0.29 | 1.65 ± 0.27 |
| [$^{18}$F]**12b** (log P = 3.07) | | | | |
| organ | 2 min | 30 min | 1 h | 2 h |
| blood | 3.28 ± 0.63 | 3.28 ± 0.57 | 3.22 ± 0.19 | 3.17 ± 0.62 |
| heart | 4.21 ± 0.79 | 1.40 ± 0.17 | 1.24 ± 0.19 | 0.96 ± 0.19 |
| muscle | 1.97 ± 1.15 | 0.61 ± 0.10 | 0.62 ± 0.07 | 0.39 ± 0.14 |
| lung | 4.64 ± 0.76 | 2.10 ± 0.30 | 2.04 ± 0.28 | 1.72 ± 0.27 |
| kidney | 4.74 ± 1.22 | 2.90 ± 0.99 | 2.40± 0.22 | 1.80 ± 0.62 |
| spleen | 2.69 ± 0.60 | 1.22 ± 0.04 | 0.95 ± 0.04 | 1.02 ± 0.15 |
| liver | 25.8 ± 2.80 | 14.8 ± 4.12 | 10.2 ± 4.00 | 9.14 ± 3.24 |
| skin | 1.24 ± 0.29 | 1.40 ± 0.23 | 0.95 ± 0.11 | 0.60 ± 0.17 |
| brain | 4.55 ± 0.82 | 0.42 ± 0.13 | 0.37 ± 0.02 | 0.38 ± 0.07 |
| bone | 1.50 ± 0.16 | 0.66 ± 0.12 | 0.65 ± 0.09 | 0.82 ± 0.15 |
| [$^{18}$F]**14b** (log P = 3.18) | | | | |
| organ | 2 min | 30 min | 1 h | 2 h |
| blood | 5.72 ± 0.51 | 2.97 ± 0.10 | 2.51 ± 0.35 | 2.35 ± 0.39 |
| heart | 9.97 ± 1.51 | 1.49 ± 0.14 | 1.04 ± 0.07 | 0.84 ± 0.10 |
| muscle | 0.79 ± 0.24 | 0.67 ± 0.10 | 0.51 ± 0.08 | 0.42 ± 0.05 |
| lung | 8.38 ± 1.28 | 2.26 ± 0.25 | 1.26 ± 0.90 | 1.47 ± 0.19 |
| kidney | 12.4 ± 2.37 | 2.68 ± 0.08 | 2.53 ± 0.21 | 2.02 ± 0.50 |
| spleen | 4.61 ± 0.76 | 1.39 ± 0.14 | 1.13 ± 0.07 | 1.17 ± 0.17 |
| liver | 23.2 ± 3.53 | 13.8 ± 0.92 | 8.13 ± 1.69 | 6.58 ± 0.43 |
| skin | 0.68 ± 0.17 | 1.41 ± 0.24 | 1.28 ± 0.06 | 0.68 ± 0.18 |
| brain | 6.78 ± 1.16 | 1.57 ± 0.13 | 0.77 ± 0.07 | 0.42 ± 0.03 |
| bone | 1.51 ± 0.34 | 0.64 ± 0.04 | 0.56 ± 0.10 | 0.70 ± 0.11 |

[a] Percent dose/g, avg of three mice ± SD.

both compounds, and the specific activity at the end of synthesis was 600−1300 mCi/$\mu$mol for [$^{18}$F]**12a** and ~600 mCi/$\mu$mol for [$^{18}$F]**12b** (radiochemical purity > 99%, radiochemical yield ~ 20%, decay corrected). The purified product showed an HPLC profile consistent with the "cold" carrier (Figure 2). To obtain [$^{18}$F]**14a** and [$^{18}$F]**14b**, the desired products were obtained in a one step reaction from **22a** and **22b**, respectively. The crude product was purified by HPLC. The procedure took 60 min for both compounds, and the specific activity at the end of synthesis was 1100−4600 mCi/$\mu$mol for [$^{18}$F]**14a** and 980−4000 mCi/$\mu$mol for [$^{18}$F]**14b** (radiochemical purity > 97%, radiochemical yield ~ 30%, decay corrected).

**Biological Evaluation.** The binding affinities ($K_i$, nM) of the diphenylacetylene compounds are evaluated via competition with [$^{125}$I]**4** binding for A$\beta$ plaques, and the results are presented in Table 1. Most of these derivatives showed excellent binding affinities toward A$\beta$ plaques. The presence of a nucleophilic group such as amino or hydroxy, attached directly to one of the phenyl rings, is necessary but not sufficient for these structures to show desirable binding characteristics. By comparing the $K_i$ values for the core structures (left-hand side of the table), it is clear that diphenylacetylene (**9**) without any substituents showed a moderate affinity (175 ± 35 nM). Simultaneously introducing $NH_2$ and OH groups (**9a**) at the 4-position on both phenyl rings increased the binding affinity ($K_i$ = 106 ± 6 nM). However, adding an *N*-methyl group to the amine moiety (**9b**) increased the binding affinity ($K_i$ = 1.5 ± 0.1 nM) about 100-fold. A comparable increase in binding affinity is also observed when the OH group in **9a** is replaced by an OMe group (**9e**; $K_i$ = 2.9 ± 0.4 nM). The introduction of a methyl group to the $NH_2$ or OH group plays a critical role in improving the binding affinities of PEGylated derivatives as well (Table 1). Compounds **11a** and **11b**, having an unsubstituted amino group, showed $K_i$ values of 12 and 21.5 nM, respectively. In comparison, their *N*-methylamino analogs, **12a** and **12b**, have $K_i$ values of 1.2 and 1.9 nM, respectively. This significant improvement in binding affinities may be attributed to the increase in lipophilicity of the molecule, with the introduction of the methyl group. However, adding one more methyl group to the amine moiety, that is, the *N*,*N*-dimethylamino derivatives, did not bring about any appreciable change in the binding properties compared to the monomethyl derivatives. The FPEGylated compound **17**, where the nucleophilic group is OH, however, showed a comparatively lower binding affinity ($K_i$ = 16.5 ± 3.5, see Table 1). Consistent with the stilbene series of ligands,[28,31] the hydroxyl substitution of the fluoro group at one end of phenyl ring by a pegylated chain did not affect the binding affinity toward A$\beta$ plaques (**20a**, **23a** vs **12a** and **14a**; **20b** and **23b** vs **12b** and **14b**). It is important to note that these seemingly extremely simple diphenylacetylenes appeared to bind $\beta$-sheets formed by A$\beta$ peptide aggregates. The binding affinity of such simple diphenylacetylenes to peptide aggregates has not been reported before.

Based on the encouraging binding data obtained with **12a**, **12b**, **14a**, and **14b**, we chose to further carry out the biological

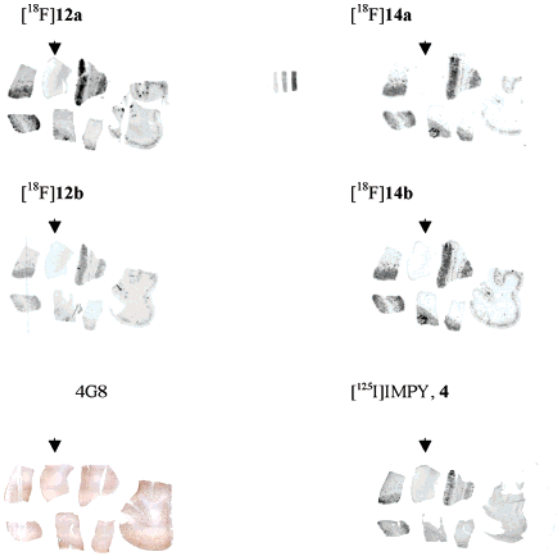


**Figure 3.** In vitro autoradiography of macroarray brain sections constructed from six postmortem AD cases plus one control (marked by arrowhead). An autoradiogram of a series standards is included for comparison. Section labeling was carried out with four $^{18}$F-labeled diphenylacetylenes. Immunohistochemistry stained with 4G8 confirmed the plaque presence in the sections. [$^{125}$I]IMPY, **4**, a well characterized SPECT ligand[35] targeting A$\beta$ plaques, was included for comparison. Clearly, the A$\beta$ plaques can be visualized for all four $^{18}$F diphenylacetylenes with low background labeling.

evaluations using $^{18}$F-labeled diphenylacetylenes as probes for A$\beta$ aggregates. All of the diphenylacetylenes measured under the experimental conditions showed relatively high partition coefficients (P.C. = 3.07−3.48), a reflection for the lipophilic property of the $^{18}$F diphenylacetylenes. Nonetheless, biodistribution studies done in the normal mice (Table 2) clearly indicated that all four diphenylacetylenes, [$^{18}$F]**12a**, **12b**, **14a**, and **14b**, readily penetrated intact blood−brain barrier showing excellent initial brain uptakes (4.42, 4.55, 5.41, and 6.78% dose/g for [$^{18}$F]**12a**, **12b**, **14a**, and **14b**, respectively, at 2 min after a tracer injection). The high brain uptakes were subsequently followed by rapid washouts (except [$^{18}$F]**14a**) with less than 1% dose/g remaining in the brain at 2 h after injection (Table 2). The difference in brain kinetics between chain length of PEG was also noted: $n = 3$ ligands [$^{18}$F]**12b** and [$^{18}$F]**14b** exhibited faster brain washouts as compared to $n = 2$ ligands, [$^{18}$F]**12a** and [$^{18}$F]**14a**. The brain washout for *N*,*N*-dimethylamino ligands, that is, [$^{18}$F]**14a** and [$^{18}$F]**14b**, was also slower as compared to *N*-methylamino ligands, that is, [$^{18}$F]**12a** and [$^{18}$F]**12b** (Table 2). The in vivo defluorination, as reflected by the bone uptake, for all four diphenylacetylene probes is low; particularly for probes with a longer PEG unit, that is, [$^{18}$F]-**12b** and [$^{18}$F]**14b**, the bone uptake was low (<1% dose/g at 2 h after injection). Consistently, blood levels for [$^{18}$F]**12a** and [$^{18}$F]**14a** ligands appeared to be higher than [$^{18}$F]**12b** and [$^{18}$F]-**14b**, and the blood activity was sustained throughout the experimental period (up to 2 h). Comparing *N*,*N*-dimethylamino with *N*-methylamino ligands, we also noted that the latter showed better and faster kinetics. A good initial brain uptake combined with a rapid washout in normal mouse brain (presumably no A$\beta$ plaques for extra binding of these probes) is a highly desirable property for A$\beta$ plaque targeting imaging agents similar to that reported for stilbene[28] or styrylpyridine analogs.[30] The diphenylacetylene probes reported here, especially [$^{18}$F]-**12b** and [$^{18}$F]**14b**, met the criteria and could be favorably considered as potential imaging agents targeting A$\beta$ plaques in vivo.

We carefully constructed human macro-array sections from six confirmed AD cases plus one control subject. After sectioning, adjacent sections would reflect comparable pathophysiology. In vitro film autoradiography was carried out with $^{18}$F-labeled diphenylacetylene probes and reported using these brain sections. Consistent with 4G8 (antibody for A$\beta$) immunohistochemical labeling, four diphenylacetylene probes, [$^{18}$F]-**12a**, **12b**, **14a**, and **14b**, all exhibited distinctive and matching plaque labeling (Figure 3) with minimal background labeling. The control case (marked by the arrowhead, Figure 3) was clearly void of any notable A$\beta$ labeling, suggesting the specificity of plaque labeling with these novel $^{18}$F-labeled diphenylacetylene probes. Furthermore, [$^{125}$I]IMPY, **4**, a well characterized SPECT imaging agent for amyloid plaques,[35] displayed a similar pattern of A$\beta$ plaque labeling on these array sections. These results confirmed the specific binding of these diphenylacetylene probes for A$\beta$ plaques. To further characterize the specific nature of plaque binding, we chose [$^{18}$F]**14b** to carry out a direct in vitro binding assay using AD brain homogenates. As expected, [$^{18}$F]**14b** displayed a specific and a saturable high binding (data not shown).

In conclusion, a new series of novel $^{18}$F-labeled diphenylacetylene derivatives, containing an end-capped fluoropolyethylene glycol ($n = 2$ and $n = 3$), were successfully prepared as potential PET imaging agents for AD. These fluorinated diphenylacetylenes displayed excellent binding affinities to A$\beta$ plaques ($K_i$ in the nM range). The radiofluorinated probes showed desirable in vivo kinetic properties in mouse brain. A specific plaque-labeling signal was clearly indicated by these probes in postmortem AD brain sections as well as in brain tissue homogenates. Taken together, the results suggest that novel diphenylacetylene series ligands could be potentially useful for in vivo PET imaging of A$\beta$ plaques in living human brain.

**Acknowledgment.** This work was supported by grants from the National Institutes of Health (AG022559 to H.F.K). The authors thank Pathology Core laboratories at Children's Hospital of Philadelphia to assemble the human macro-array brain sections. The authors also thank Drs. Daniel Skovronsky and Rajesh Manchanda for their helpful discussion.

**Supporting Information Available:** Schemes and procedures for the synthesizing intermediates **10**(**a**,**b**) and **18**(**a**,**d**) mentioned in the paper; the purity and HPLC data (using normal as well as reverse phase columns) of compounds **9**(**a**,**b**), **11**(**a**,**b**), **12**(**a**,**b**), **14**(**a**,**b**), **17**, **19b**, **20**(**a**,**b**), and **23**(**a**,**b**), which were used for the biological evaluations. This material is available free of charge via the Internet at http://pubs.acs.org.

## References

(1) Hardy, J.; Selkoe, D. J. The amyloid hypothesis of Alzheimer's disease: Progress and problems on the road to therapeutics. *Science* **2002**, *297*, 353−356.
(2) Hardy, J. Has the amyloid cascade hypothesis for Alzheimer's disease been proved? *Curr. Alzheimer Res.* **2006**, *3*, 71−73.
(3) Armstrong, R. A. Plaques and tangles and the pathogenesis of Alzheimer's disease. *Folia Neuropathol.* **2006**, *44*, 1−11.
(4) Golde, T. E. The Abeta hypothesis: Leading us to rationally-designed therapeutic strategies for the treatment or prevention of Alzheimer disease. *Brain Pathol.* **2005**, *15*, 84−87.
(5) Goedert, M.; Spillantini, M. G. A century of Alzheimer's disease. *Science* **2006**, *314*, 777−781.
(6) Roberson, E. D.; Mucke, L. 100 years and counting: Prospects for defeating Alzheimer's disease. *Science* **2006**, *314*, 781−784.

(7) Braak, H.; Alafuzoff, I.; Arzberger, T.; Kretzschmar, H.; Del Tredici, K. Staging of Alzheimer disease-associated neurofibrillary pathology using paraffin sections and immunocytochemistry. *Acta Neuropathol.* **2006**, *112*, 389−404.
(8) Selkoe, D. J. The origins of Alzheimer disease: A is for amyloid. *JAMA, J. Am. Med. Assoc.* **2000**, *283*, 1615−1617.
(9) Selkoe, D. J. Alzheimer's disease: Genes, proteins, and therapy. *Physiol. Rev.* **2001**, *81*, 741−766.
(10) Blennow, K.; Zetterberg, H. Pinpointing plaques with PIB. *Nat. Med.* **2006**, *12*, 753−754.
(11) Mathis, C. A.; Wang, Y.; Klunk, W. E. Imaging $\beta$-amyloid plaques and neurofibrillary tangles in the aging human brain. *Curr. Pharm. Des.* **2004**, *10*, 1469−1492.
(12) Nichols, L.; Pike, V. W.; Cai, L.; Innis, R. B. Imaging and in vivo quantitation of beta-amyloid: An exemplary biomarker for Alzheimer's disease? *Biol. Psychiatry* **2006**, *59*, 940−947.
(13) Schmidt, B.; Braun, H. A.; Narlawar, R. Drug development and PET-diagnostics for Alzheimer's disease. *Curr. Med. Chem.* **2005**, *12*, 1677−1695.
(14) Huddleston, D. E.; Small, S. A. Technology Insight: Imaging amyloid plaques in the living brain with positron emission tomography and MRI. *Nat. Clin. Pract. Neurol.* **2005**, *1*, 96−105.
(15) Klunk, W. E.; Engler, H.; Nordberg, A.; Wang, Y.; Blomqvist, G.; Holt, D. P.; Bergstrom, M.; Savitcheva, I.; Huang, G.-f.; Estrada, S.; Ausen, B.; Debnath, M. L.; Barletta, J.; Price, J. C.; Sandell, J.; Lopresti, B. J.; Wall, A.; Koivisto, P.; Antoni, G.; Mathis, C. A.; Langstrom, B. Imaging brain amyloid in Alzheimer's disease with Pittsburgh compound-B. *Ann. Neurol.* **2004**, *55*, 306−319.
(16) Verhoeff, N. P.; Wilson, A. A.; Takeshita, S.; Trop, L.; Hussey, D.; Singh, K.; Kung, H. F.; Kung, M.-P.; Houle, S. In vivo imaging of Alzheimer disease beta-amyloid with [11C]SB-13 PET. *Am. J. Geriatr. Psychiatry* **2004**, *12*, 584−595.
(17) Shoghi-Jadid, K.; Small, G. W.; Agdeppa, E. D.; Kepe, V.; Ercoli, L. M.; Siddarth, P.; Read, S.; Satyamurthy, N.; Petric, A.; Huang, S. C.; Barrio, J. R.; Liu, J.; Flores-Torres, S.; Cole, G. M. Localization of neurofibrillary tangles and beta-amyloid plaques in the brains of living patients with Alzheimer disease: Binding characteristics of radiofluorinated 6-dialkylamino-2-naphthylethylidene derivatives as positron emission tomography imaging probes for beta-amyloid plaques in Alzheimer disease. *Am. J. Geriatr. Psychiatry* **2002**, *10*, 24−35.
(18) Small, G. W. Diagnostic issues in dementia: neuroimaging as a surrogate marker of disease. *J. Geriatr. Psychiatry Neurol.* **2006**, *19*, 180−185.
(19) Newberg, A. B.; Wintering, N. A.; Plossl, K.; Hochold, J.; Stabin, M. G.; Watson, M.; Skovronsky, D.; Clark, C. M.; Kung, M. P.; Kung, H. F. Safety, biodistribution, and dosimetry of 123I-IMPY: A novel amyloid plaque-imaging agent for the diagnosis of Alzheimer's disease. *J. Nucl. Med.* **2006**, *47*, 748−754.
(20) Rentz, D. M.; Becker, J. A.; Moran, E.; Sperling, R. A.; Manning, L.; Bonab, A.; Mathis, C. A.; Klunk, W.; Fischman, A. J.; Johnson, K. A. Amyloid imaging in AD, MCI, and highly intelligent older adults with Pittsburgh compound-B (PIB). *J. Nucl. Med.* **2006**, 289p (abstract).
(21) Villemagne, V. L.; Ng, S.; Gong, S. J.; Ackermann, U.; Pike, K.; Savage, G.; Klunk, W.; Mathis, C.; Masters, C. L.; Rowe, C. C. 11C-PIB PET imaging in the differential diagnosis of dementia. *J. Nucl. Med.* **2006**, 74p (abstract).
(22) Edison, P.; Archer, H. A.; Hinz, R.; Hammers, A.; Pavese, N.; Tai, Y. F.; Hotton, G.; Cutler, D.; Fox, N.; Kennedy, A.; Rossor, M.; Brooks, D. J. Amyloid, hypometabolism, and cognition in Alzheimer disease. An [11C]PIB and [18F]FDG PET study. *Neurology* **2006**.
(23) Barrio, J. R.; Huang, S.-C.; Cole, G.; Satyamurthy, N.; Petric, A.; Phelps, M. E.; Small, G. PET imaging of tangles and plaques in Alzheimer's disease with a highly hydrophobic probe. *J. Labelled. Compd. Radiopharm.* **1999**, *42* (Suppl. 1), S194.
(24) Shoghi-Jadid, K.; Barrio, J. R.; Kepe, V.; Huang, S. C. Exploring a mathematical model for the kinetics of beta-amyloid molecular imaging probes through a critical analysis of plaque pathology. *Mol. Imaging Biol.* **2006**, *8*, 151−162.
(25) Kepe, V.; Barrio, J. R.; Huang, S. C.; Ercoli, L.; Siddarth, P.; Shoghi-Jadid, K.; Cole, G. M.; Satyamurthy, N.; Cummings, J. L.; Small, G. W.; Phelps, M. E. Serotonin 1A receptors in the living brain of Alzheimer's disease patients. *Proc. Natl. Acad. Sci. U.S.A.* **2006**, *103*, 702−707.
(26) Small, G. W.; Kepe, V.; Ercoli, L. M.; Siddarth, P.; Bookheimer, S. Y.; Miller, K. J.; Lavretsky, H.; Burggren, A. C.; Cole, G. M.; Vinters, H. V.; Thompson, P. M.; Huang, S. C.; Satyamurthy, N.; Phelps, M. E.; Barrio, J. R. PET of brain amyloid and tau in mild cognitive impairment. *N. Engl. J. Med.* **2006**, *355*, 2652−2663.
(27) Mathis, C. A.; Holt, D. P.; Wang, Y.; Huang, G. F.; Debnath, M. L.; Klunk, W. E. $^{18}$F-Labeled thioflavin-T analogs for amyloid assessment. *J. Nucl. Med.* **2002**, *43*, 166P.
(28) Zhang, W.; Oya, S.; Kung, M. P.; Hou, C.; Maier, D. L.; Kung, H. F. F-18 PEG stilbenes as PET imaging agents targeting A$\beta$ aggregates in the brain. *Nucl. Med. Biol.* **2005**, *32*, 799−809.
(29) Zhang, W.; Oya, S.; Kung, M. P.; Hou, C.; Maier, D. L.; Kung, H. F. F-18 stilbenes as PET imaging agents for detecting beta-amyloid plaques in the brain. *J. Med. Chem.* **2005**, *48*, 5980−5988.
(30) Zhang, W.; Kung, M. P.; Oya, S.; Hou, C.; Kung, H. F. (18)F-Labeled styrylpyridines as PET agents for amyloid plaque imaging. *Nucl. Med. Biol.* **2007**, *34*, 89−97.
(31) Stephenson, K. A.; Chandra, R.; Zhuang, Z. P.; Hou, C.; Oya, S.; Kung, M. P.; Kung, H. F. Fluoro-pegylated (FPEG) imaging agents targeting A$\beta$ aggregates. *Bioconjug. Chem.* **2007**, *18*, 238−246.
(32) Kung, M.-P.; Hou, C.; Zhuang, Z.-P.; Cross, A. J.; Maier, D. L.; Kung, H. F. Characterization of IMPY as a potential imaging agent for $\beta$-amyloid plaques in double transgenic PSAPP mice. *Eur. J. Nucl. Med. Mol. Imaging* **2004**, *31*, 1136−1145.
(33) Mohamed, Ahmed, M. S.; Mori, A. Sonogashira coupling with aqueous ammonia directed to the synthesis of azotolane derivatives. *Tetrahedron* **2004**, *60*, 9977−9982.
(34) Elangovan, A.; Wang, Y.-H.; Ho, T.-I. Sonogashira coupling reaction with diminished homocoupling. *Org. Lett.* **2003**, *5*, 1841−1844.
(35) Kung, M.-P.; Hou, C.; Zhuang, Z.-P.; Skovronsky, D.; Kung, H. F. Binding of two potential imaging agents targeting amyloid plaques in postmortem brain tissues of patients with Alzheimer's disease. *Brain Res.* **2004**, *1025*, 89−105.

JM070090J